Green Chemistry

PAPER

View Article Online
View Journal | View Issue

Cite this: *Green Chem.*, 2024, **26**, 2793

Bio-based solvents as a sustainable alternative to develop a multiproduct biorefinery process from archaebacteria *Halobacterium salinarum* R1†

Mariam Kholany,[a] Inês P. E. Macário,[a,b] Telma Veloso,[a,b] Letícia S. Contieri,[a,c] Bárbara M. C. Vaz,[a] Joana L. Pereira,[b] Cláudia Nunes,[a] João A. P. Coutinho,[a] Maurício A. Rostagno,*[c] Sónia P. M. Ventura*[a] and Leonardo M. de Souza Mesquita*[c]

Received 11th October 2023,
Accepted 19th January 2024

DOI: 10.1039/d3gc03870j

rsc.li/greenchem

This study delves into an innovative biorefinery approach to extract multiple high-value compounds from a single biomass source, *Halobacterium salinarum* R1, a resilient halophilic microorganism. By using bio-based solvents, namely an aqueous solution of gamma-valerolactone (GVL) and ethanol, a simple and efficient pipeline approach was developed, recovering unique pigments, including C_{50} bacterioruberin, as well as two additional fractions consisting of protein and polysaccharides. The process is based on sustainable engineering and green chemistry principles, providing a viable alternative to replacing non-renewable solvents. The study addresses environmental concerns by employing bio-based solvents while presenting a cost-effective and sustainable solution. This approach contributes to developing a high-performance and sustainable alternative, promoting the development of a blue bioeconomy.

Introduction

Growing awareness and global demand for sustainable energy, food, and other products propel a significant shift from a fossil fuel-based economy that relies on finite resources towards a bioeconomy based on biomass.[1,2] While terrestrial biomass is the driving feedstock for the "green bioeconomy", largely untapped marine resources offer great potential to drive the development of sustainable products through a "blue bioeconomy". These resources, including macroalgae, microalgae, and other marine microorganisms, are best known for producing biomaterials and biofuels due to their high fat and polysaccharide content.[3,4] Nonetheless, new fields of application are being driven by the production of several natural bio-active molecules of paramount relevance in the food, cosmetic, medical, and biopharmaceutical industries.[5] Microorganisms have several advantages over other biomass sources, namely algae and terrestrial plants, for producing and extracting value-added components. They present faster growth rates and higher biomass yields than plants or algae, making them more efficient feedstocks of bioactive compounds.

Additionally, microorganisms can be easily cultured in controlled environments, allowing for the automation of the cultivation while providing reproducibility between batches, ensuring a consistent and reliable biomass supply. This level of control and reproducibility is not always possible with plant-based biomass sources, which can be affected by factors such as climate, soil conditions, and seasons.[6] In particular, archaea, also termed archaebacteria, constitute an underexplored resource with great potential for producing novel metabolites due to their adaptation to extreme environmental conditions and unique metabolic pathways.[3] The extremophile profile associated with several archaea generally allows them to be cultivated under extreme non-sterile conditions based on inexpensive feedstocks, reducing the risk of culture contamination by other microorganisms, thus, simplifying the cultivation process and lowering operating costs.[3] Halobacteria (or haloarchaea), found worldwide in hypersaline environments, are natural producers of numerous high-demand products, namely proteins, poly(3-hydroxybutyrate), polyhydroxyalkanoates (PHAs), and carotenoids.[7] Most halophilic archaea synthesize bacterioruberin, a C50 carotenoid, in contrast to the C40 carotenoids found in most natural sources such as

[a]*CICECO – Aveiro Institute of Materials, Department of Chemistry, University of Aveiro, Campus Universitário de Santiago, 3810-193 Aveiro, Portugal. E-mail: spventura@ua.pt*
[b]*Department of Biology & CESAM, University of Aveiro, 3810-193 Aveiro, Portugal*
[c]*Multidisciplinary Laboratory of Food and Health (LabMAS), School of Applied Sciences (FCA), University of Campinas, Rua Pedro Zaccaria 1300, 13484, Brazil. E-mail: mesquitalms@gmail.com, mauricio.rostagno@fca.unicamp.br*

† Electronic supplementary information (ESI) available. See DOI: https://doi.org/10.1039/d3gc03870j

bacteria, algae, fungi, and plants.[8] Compared to the nine pairs of conjugated double bonds in the C40-carotenoids, bacterioruberin contains 13 conjugated double bonds and four hydroxyl groups, making it a superior antioxidant and consequently of a higher biological value.[9] Usually, carotenoids display high protection against intensive light, gamma irradiation, oxidative stress, and DNA-damaging agents, including radiography, UV irradiation, and H_2O_2 exposure.[10,11] These features grant bacterioruberin interest in several new applications in the food, cosmetic, medical, and pharmaceutical sectors, which until now was not been commercially explored.

Following the concepts of circular economy and integrated biorefineries, marine biomass fractions should be fully exploited. Feasibility studies suggest that focusing biomass valorization on a single product is not cost-effective.[12,13] A multiproduct biorefinery will maximize the value of raw materials and minimize waste generation while mitigating production costs, thus increasing the overall value of biomass.[14] When targeting carotenoid recovery from biomass, non-renewable solvents like hexane, ether, or acetone are often used. At best, ethanol : hexane mixtures are used,[15,16] whereas water-soluble components such as proteins and carbohydrates are often discarded or undervalued. However, these fractions should be addressed in the biorefinery design as they constitute sustainable sources of general commodities or specialty compounds that can be easily integrated into the same process while enhancing their value. Generally, carbohydrates derived from marine biomass have shown promising potential in various applications such as for producing biofuels,[17] as pharmaceuticals, where they can serve as intermediates for antivirus and anti-cancer drugs,[18] and in the food industry, offering functional properties like blood sugar-lowering effects.[19] Marine proteins are often valorized for animal feed or food applications. The development, application, and potential of integrated algal biorefineries are well summarized across recent reviews.[20–22] The same principle can be applied to other under-valorized marine feedstocks, as recently demonstrated for the sequential recovery of astaxanthin, proteins, chitin, and calcium carbonate from crustacean wastes.[23]

Furthermore, there is a growing market shift towards using greener alternative solvents in downstream processes. This shift was prompted by an increasing understanding of the harmful effects of conventional solvents on human health and the environment.[24] An ideal solvent should have minimal toxicity, high biodegradability, and be sourced from renewable sources whenever possible while having high dissolving power and selectivity for the target molecules. Because standard organic solvents commonly used for carotenoid extraction do not match these criteria, efforts should be in find suitable alternatives.[25]

This study proposes a comprehensive biorefinery design for valorizing different molecular fractions from the red archaea *Halobacterium salinarum* R1, emphasizing the highest valued molecule – bacterioruberin. The downstream processing strategy aims to increase archaea production's economic feasibility by maximizing the biomolecules' recovery. Other studies reported the extraction of bacterioruberin using organic solvents such as acetone or methanol,[26,27] and aqueous solutions of surfactants.[28] However, the different nature of the biomass substrate and the extraction conditions used prevent a direct comparison to determine the best extraction media. To address this limitation, here, several conventional and neoteric solvents belonging to different classes were evaluated as representative examples of extraction media (water, aqueous surfactant solutions, ionic liquids, and organic solvents). Each of these solvents offers distinct extraction efficiencies, and their choice has traditionally been guided by this metric. However, the merits of a solvent extend beyond just extraction performance. Sustainability, environmental footprint, and resource efficiency are pivotal. In this context, biosolvents emerge as increasingly important. Derived from renewable resources, these solvents offer a multitude of benefits. They are characterized by their reduced environmental footprint and biodegradability, contributing significantly to sustainability.[29] Focus is placed on the water as a solvent through additives to extract and stabilize the hydrophobic bacterioruberin. These can create milder extraction conditions and allow the simultaneous extraction of hydrophobic and hydrophilic compounds.

Eventually, aqueous gamma-valerolactone (GVL) solutions were selected as extraction media for their ability to recover bacterioruberin. GVL is considered a versatile bio-based solvent for extracting valuable compounds from biomass. This solvent possesses several desirable properties, including its low toxicity and biodegradability, and can be produced from biomass.[29] Moreover, GVL does not form azeotropes with water, which may facilitate the separation of the solvents.[30] Its low volatility also presents a safer solvent to use in industrial processes. This bio-solvent is also approved as an additive in food, cosmetics, and agrochemicals.[29,31,32] Thus, using a GVL aqueous solution, the extraction conditions were optimized, and the thermal stability of the pigment was evaluated. Finally, the separation of the proteins and carbohydrates co-extracted with the pigment was achieved using induced ethanol precipitation, followed by a temperature-based fractionation. In the end, the goal was to obtain three ready-to-market products, providing the first application of an integrated multiproduct biorefinery approach focused on Archaea and opening the door for valorizing this unique class of marine biomass.

Materials and methods

Chemicals

Halobacterium salinarum R1 (DSM 671) was purchased from DSMZ German Collection (Leibniz Institute, Germany). For *H. salinarum* R1 culturing, yeast extract, tryptone was acquired from Organotechnie, NaCl from J. T. Baker, $MgSO_4{\cdot}7H_2O$, $CaCl_2$ from VWR Chemicals, $MgCl_2{\cdot}6H_2O$ from Biochem Chemopharma, and KCl and glycerol from JMGS. The anionic surfactant sodium dodecylsulfate (SDS, pharma grade) was

supplied by Panreac. The ammonium ILs, *n*-octyltrimethylammonium bromide $[N_{1,1,1,8}]Br$ (98 wt%) and decyltrimethylammonium bromide $[N_{1,1,1,10}]Br$ (99 wt%) were aquired from TCI, and dodecyltrimethylammonium bromide $[N_{1,1,1,12}]Br$ (99 wt%), tetradecyltrimethylammonium bromide $[N_{1,1,1,4}]Br$ (98 wt%) were purchased from Alfa Aesar. The non-ionic surfactants Tween 20 and Tween 80 were aquired from Acros Organics and Sigma-Aldrich, respectively. The non-tensioactive ILs tested, 1-ethyl-3-methylimidazolium acetate $[C_2mim][CH_3CO_2]$ (97 wt%) and 1-butyl-3-methylimidazolium acetate acetate $[C_4mim][CH_3CO_2]$ (97 wt%) were both obtained from Iolitec. Gamma-valerolactone (GVL, 98 wt%) and cyrene (99 wt%) were purchased from ThermoScientific and Sigma-Aldrich, respectively. The conventional organic solvents, methanol (HPLC grade), acetone (100 wt%), and ethanol (analytical grade), were obtained from Fisher Scientific. Dichloromethane (99.9 wt%) and ethyl acetate (analytical grade) were purchased from Honeywell, *n*-hexane (99 wt%) from Normapur, and diethyl ether supplied from Panreac.

Archaea cultivation

Halobacterium salinarum was cultured, as described in Kalenov *et al.*,[33] with some modifications to maximize the yields of the production of bacterioruberin. The culture medium consists of a basic salt solution with the following mineral components: 250 g L^{-1} NaCl, 20 g L^{-1} $MgSO_4{\cdot}7H_2O$, 3 g L^{-1} KCl, 3 g L^{-1} nacitrate, and 0.2 g L^{-1} $CaCl_2$. The following organic compounds were added to this solution: 5.0 g L^{-1} tryptone, 2.0 g L^{-1} yeast extract, and 1.0 g L^{-1} glycerol. The medium was sterilized at 121 °C for 15 min.

Pre-inoculums were set up before increasing production scale in sterile 100 mL Erlenmeyers with 25 mL of culture medium, and *H. salinarum* colonies scraped from a Petri dish; these cultures were kept to grow in a shaking incubator SH Maxi (Controltecnica Instruments, Spain) at 150 rpm, 500 lux provided by cool white lights, at 38.5 °C, during 72 h. Culturing scale was increased by adding 4% (v/v) of pre-inoculum to a sterile 1 L Erlenmeyer with 500 mL of culture medium, which was incubated under the same conditions for 120 h. *H. salinarum* growth was confirmed using optical density at 600 nm (UV 1800 Shimadzu spectrophotometer, Japan), and the biomass was harvested through centrifugation at 4111*g* for 30 min, at room temperature (Eppendorf 5810 R), then stored at −20 °C until bacterioruberin extraction.

Cell disruption and solid–liquid extraction

Cell disruption and solid–liquid extraction were performed simultaneously following a previously developed protocol.[28] A total of 23 alternative and conventional solvents were used, namely water, conventional organic solvents, and aqueous solutions of tension active solvents (ionic liquids (IL) and surfactants), non-tension active ILs and bio-based solvents, to comprehensively assess their ability to release bacterioruberin (the most valuable compound) from the biomass. An initial concentration of 250 mM was selected for the surfactant and IL solutions and up to 50% v/v for the organic solvents. Unless otherwise specified, all extractions were carried out at a fixed solid–liquid ratio (SLR) of 0.15 $g_{wet\ biomass}\ mL_{solvent}^{-1}$ under a constant vertical rotation of 80 rpm in a shaker (IKA Trayster Digital), for 30 min, protected from light exposure and at room temperature. Finally, a centrifugation step was performed at 16 200*g* for 15 min in a VWR Microstar 17 centrifuge at room temperature. The resulting supernatant was recovered, and the biomass debris was discarded. All the assays were done in triplicate.

The quantification of bacterioruberin was determined using a UV-Vis microplate reader (Synergy HT microplate reader-BioTek). The absorption spectra of the extracts were analyzed between 350 and 700 nm, and the bacterioruberin content was determined in terms of bacterioruberin extraction yield expressed by eqn (1) using a calibration curve at the maximum peak of absorbance observed, 504 nm (Fig. S1 – ESI†). The bacterioruberin standard used to determine the calibration curves was attained by preparative thin-layer chromatography (TLC), as previously reported by us.[28]

$$\text{Yield of extraction}\left(mg_{bacterioruberin}\ g_{wet\ biomass}^{-1}\right) = \frac{[\text{Bacterioruberin}] \times \text{volume}}{\text{mass}} \quad (1)$$

Here "[Bacterioruberin]" corresponds to the concentration of bacterioruberin in the extract (mg mL^{-1}), "volume" is the volume of solvent (mL) and "mass" is the amount of the wet cells tested (g).

Process optimization and kinetics

The optimization of the extraction process towards maximizing the yield of bacterioruberin extraction was done by applying a central composite rotatable design (CCRD-2^3), totaling 20 extractions with six replicates at the central point, which allowed to analyze different variables simultaneously and to identify the most significant parameters and their interaction. The independent variables considered were GVL concentration in water (mM), the solid–liquid ratio (SLR, $g_{biomass}\ mL_{solvent}^{-1}$), and the system pH, and the dependent variable was the yield of extraction of bacterioruberin (yield of extraction, $mg_{carotenoids}\ g_{biomass}^{-1}$). The temperature, agitation, and extraction time were kept constant as described for the screening of solvents, *i.e.*, 25 °C, 80 rpm and 30 min, respectively. The results were statistically analyzed with a 95% confidence level. The Statistica® 14 software was used for all statistical analyses and for representing the response surfaces and contour plots. The experimental values are shown in Table S1 in ESI.† The predicted optimum conditions determined were validated in triplicate using the means of relative deviation (%).

The extraction kinetics were assessed after determining the optimal pH, SLR, and GVL concentration parameters. The kinetic data were described using the first and second-order kinetic models.[34] The first-order kinetic equation in its differential form is given by eqn (2),

$$\frac{dC_t}{dt} = k_1(C_S - C_t) \quad (2)$$

where k_1 (min^{-1}) is the first-order extraction rate constant, t (min) is the extraction time, and C_S and C_t are the bacterioruberin yield at saturation and for a specific extraction time, respectively. Integration of eqn (2) with the boundary conditions $C_t = 0$ at $t = 0$ and $C_t = C_t$ at $t = t$ gives eqn (3):

$$\ln\left(\frac{C_S}{C_S - C_t}\right) = k_1 t \quad (3)$$

where k_1 was obtained through the slope of the graph obtained by plotting ln values of C_t against t. The second-order kinetic equation for the rate of extraction can be written as per eqn (4):

$$\frac{dC_t}{dt} = k_2(C_s - C_t)^2 \quad (4)$$

where k_2 ($g_{biomass}$ $\mu g_{carotenoids}^{-1}$ min^{-1}) is the second-order extraction rate constant. After integration using the boundary conditions $C_t = 0$ at $t = 0$ and $C_t = C_t$ at $t = t$ and linearisation, the following eqn (5) is obtained:

$$\frac{t}{C_t} = \frac{t}{C_S} + \frac{1}{k_2 C_S{}^2} \quad (5)$$

By plotting t/C_t against t, the C_S and k_2 constants can be determined from the slope and intercept of the plot, respectively.

Proteins and polysaccharides recovery and quantification

Bacterioruberin was separated from the other components, namely proteins and polysaccharides, through induced precipitation using ethanol as the precipitating agent. The ethanol was added to the extract at a ratio of 1 : 4 ($V_{extract} : V_{ethanol}$) and left at 25 °C for 2 min, according to a previously reported protocol.[28] The sample was then centrifuged using a Thermo Scientific Heraeus Megafuge 16R centrifuge at 4700*g* for 15 min. This resulted in a pellet enriched in proteins and polysaccharides, which was separated from the bacterioruberin-rich supernatant. The purified supernatant was recovered, and the ethanol was evaporated, providing a bacterioruberin-rich fraction in GVL as the first product.

The recovery of two more products further valorized the obtained pellet. To this end, the pellet was resuspended in 45 mL of PBS (1×, pH 7.4), and the solution was kept at 4 °C for 24 h to induce protein precipitation while keeping the polysaccharides in the aqueous solution (supernatant). The polysaccharide-rich supernatant was recovered and characterized by derivatization to alditol acetates an analysis in GC-MS, following a previously reported protocol.[35] Protein quantification was conducted using the Bradford method, with a calibration curve previously established with bovine serum albumin (BSA) (Fig. S2 – ESI†). UV-vis spectroscopy was used for quantification, using a BioTek Synergy HT microplate reader at 595 nm (Biotek Instruments, Winooski, VT, USA).

Thermal stability of the pigment

The thermal stability of bacterioruberin extract obtained using the optimal extraction and solvent conditions (SLR 0.15, GVL 150 mM, and pH 7) was studied at three temperatures (56 °C, 76 °C, and 96 °C). Vials containing 1.5 mL of the bacterioruberin extract before and after protein precipitation were heated in a heating block for up to 5000 min, collected at different times, and immediately cooled in an ice bath to stop any reaction in the samples.[36] Afterwards, each collected vial was analyzed by UV-vis. The degradation rate constant (k_d, min^{-1}) was estimated by regression of the natural logarithm of the bacterioruberin concentration with time, assuming first-order reaction kinetics as per eqn (2), with an obtained $R_2 \geq 0.93$. In addition, the half-life time ($t_{1/2}$, min) and thermal activation energy data (E_a, kJ mol^{-1}) were obtained per eqn (6) and (7), respectively.

$$t_{1/2} = \frac{\ln(2)}{k_d} \quad (6)$$

$$k_d = Ae^{-E_a/RT} \quad (7)$$

where A is the frequency factor (min^{-1}), T is the temperature (K), and R is the gas constant (8.31 J K^{-1} mol^{-1}).

Economic analysis of the process

The economic analysis was carried out specifically for a laboratory-scale process, thus excluding costs related to energy and machinery. All costs were analyzed considering one biomass batch, corresponding to 8.4 g of dry biomass (*H. salinarum* R1). In addition, projections were made by considering a hypothetical selling price/mg for the obtained products (C_{50} – bacterioruberin: US$ 75.00; proteins: US$ 2.00, and polysaccharides-rich fractions: US$ 0.23). The biorefinery approach was divided into four main steps, and their respective costs are depicted in Table S2 (ESI†). The theoretical selling price of each obtained product was chosen considering the price of similar commercial products. However, it could vary considering their individual purity levels. Eqn (8) was applied to determine the production costs per milligram (mg) of products (coG per mg) per "*n*" batches. Eqn (9), adapted from ref. 37, estimated the process's return, incorporating five variables to calculate potential profits (return: $ per $mg_{biomass}$), taking into account the recycling of raw materials, particularly the used solvents, in subsequent extraction cycles. The concentration of products per mg of biomass (C_{prod}) is represented by eqn (2), which is based on the extraction yield achieved under optimized conditions ($mg_{products}$ $g_{biomass}^{-1}$). The selling price of the products is denoted by $prod. The cost to cultivate *H. salinarum* R1 is represented by $biomass (representing the costs of step I of the biorefinery approach – cultivation of *H. salinarum* R1), as depicted in Table S2 (ESI†). A multiplier factor (α = 0.1, 1, 5 and 10) was used to express different price scenarios to account for potential variations in the price of raw materials due to market trends or product purity.

Three distinct scenarios were evaluated regarding their costs and economic return, namely, (i) scenario I, where only one product is obtained (mixture of carotenoids, proteins, and polysaccharides), (ii) scenario II, three separated products are obtained (carotenoids, proteins, and polysaccharides), and (iii)

scenario III, where the same products are obtained, but the raw materials are reused in new extraction batches. Here, we simulated the costs considering ten extraction cycles using the same raw material, which is a feasible approach.

$$\text{Costs} = \frac{\sum_{i=n} n \times \text{materials}}{\text{mg}_{\text{products}}} \quad (8)$$

$$\text{Return}\left(\frac{\$}{\text{g}_{\text{biomass}}}\right) = [C_{\text{prod}} \times \$_{\text{prod}}] - \$_{\text{biomass}} - \left[\alpha \times \frac{\text{costs}}{\text{g}_{\text{biomass}}}\right] \quad (9)$$

Ecoscale score

The Ecoscale database was used to score the environmental impact of the biorefinery process.[38] In this analysis, penalty points were assigned based on several factors: safety, solvent, price/availability, technical setup, temperature applied in the extraction/purification process, workup, and purification steps. In addition, the Ecoscale score of other works focusing on the extraction of carotenoids using alternative solvents was performed to compare performances. These aspects were then standardized by the relative yield of carotenoids (%relative), considering 100% the highest experimental yield ($\mu g_{\text{carotenoids}}\ g_{\text{biomass}}^{-1}$) obtained. The Ecoscale score approach evaluated the same scenarios of the economic analysis. The findings were presented as a score ranging from 1 to 100, with 1 representing the least environmentally friendly process and 100 meaning the most eco-friendly process.

Results and discussion

Solvent screening for bacterioruberin extraction

Several solvents were screened in their capacity to extract bacterioruberin from the intracellular matrix of *H. salinarum* R1. Emphasis was placed on the valorization of water as a solvent using additives to solubilize and stabilize the hydrophobic bacterioruberin. The solvents were chosen as representative examples of extraction media belonging to different classes: water, aqueous surfactant solutions, ionic liquids, and organic solvents, considering previous works that showed these to be effective specifically for the extraction of carotenoids.[28,37,39] The intention at this stage is not to perform an exhaustive screening but rather to ascertain the most promising class of solvent as a platform for further optimization. Within the water-based solvents, different surfactants spanning the range from anionic (SDS), cationic ($[N_{1,1,1,x}]$Br for x = 8–14), and non-ionic (Tween 20 and 80) were selected. Additionally, aqueous solutions of acetate-based ionic liquids and bio-based organic solvents were identified due to their capacity to dissolve recalcitrant biomass[40] through the disruption of its hydrogen-bonding network as well as their role as hydrotropes,[29,41,42] thereby ensuring the solubilization of the pigment. Here, an initial concentration of 250 mM was arbitrarily considered for the surfactant solutions and up to 50% for the organic solvents. Finally, these were compared against pure organic solvents presenting a range of polarities from methanol to *n*-hexane. The results regarding bacterioruberin extraction yield are depicted in Fig. 1.

Due to the halophilic nature of *H. salinarum* R1, the presence of water in the extraction is assumed to promote cell rupture by increasing the osmotic pressure in the cell.[3] It is noticeable that the presence of water greatly influenced the success of the extraction, as evidenced by a simple comparison with the more apolar solvents, the latter presenting negligible extraction yields (except for alcohols). Additionally, the lower extraction yields of the pure aprotic polar solvents, including cyrene, GVL, and acetone, relative to the protic MeOH and EtOH, suggests that a degree of hydrogen bonding acidity is required. The role of hydrogen bonding in the extraction could also explain the greater bacterioruberin yield obtained in the $[C_2mim][CH_3COO]$ relative to the $[C_4mim]$-based IL despite the smaller apolar volume of the former. In line with a previous study,[28] all aqueous surfactant solutions displayed good extracting capabilities, irrespective of the surfactant type. Several studies[39,43] have shown that tension active molecules can promote cell disruption by spontaneously inserting the surfactant alkyl chains into the cell lipid bilayer, causing membrane swelling and lipid bilayer disruption. In this context, aqueous solutions of hydrophilic organic solvents were trialed to establish a compromise between extraction efficiency and pigment solubility through the variation in solvent properties. The addition of water in the case of ethanol, acetone, and methanol seemed to hinder the extraction capability of the system.

In contrast, adding water to the systems with low-volatility organic solvents (cyrene and GVL) enhanced the extraction significantly. Indeed, the best extraction yield was obtained using a small concentration of 250 mM of GVL in an aqueous solution. The non-linear profile in the bacterioruberin solubility relative to that of the pure solvents with the variation in the water-to-GVL ratio is not uncommon in hydrotropic systems due to the delicate chemical equilibrium established between water, the hydrotrope, and solute.[44] Promising results were obtained for 250 mM of GVL with an increased extraction yield compared to the conventional ethanol extraction method, indicating significant potential as an extractant. As a result, the following work was performed using aqueous solutions of GVL.

Optimization of the solid–liquid extraction

Having identified aqueous solutions of GVL as the most promising solvent mixture for the extraction of bacterioruberin, here aqueous solutions of GVL, the operational extraction conditions were further optimized based on a central composite rotatable design (CCRD – 2^3 + axial and central points) before an explicit consideration of the extraction kinetics at room temperature. Although protein and polysaccharide recovery are discussed further on, the optimization is focused on the recovery of the most valuable compound/fraction, the bacterioruberin. The central composite rotatable design is composed of three independent variables, namely GVL concentration in

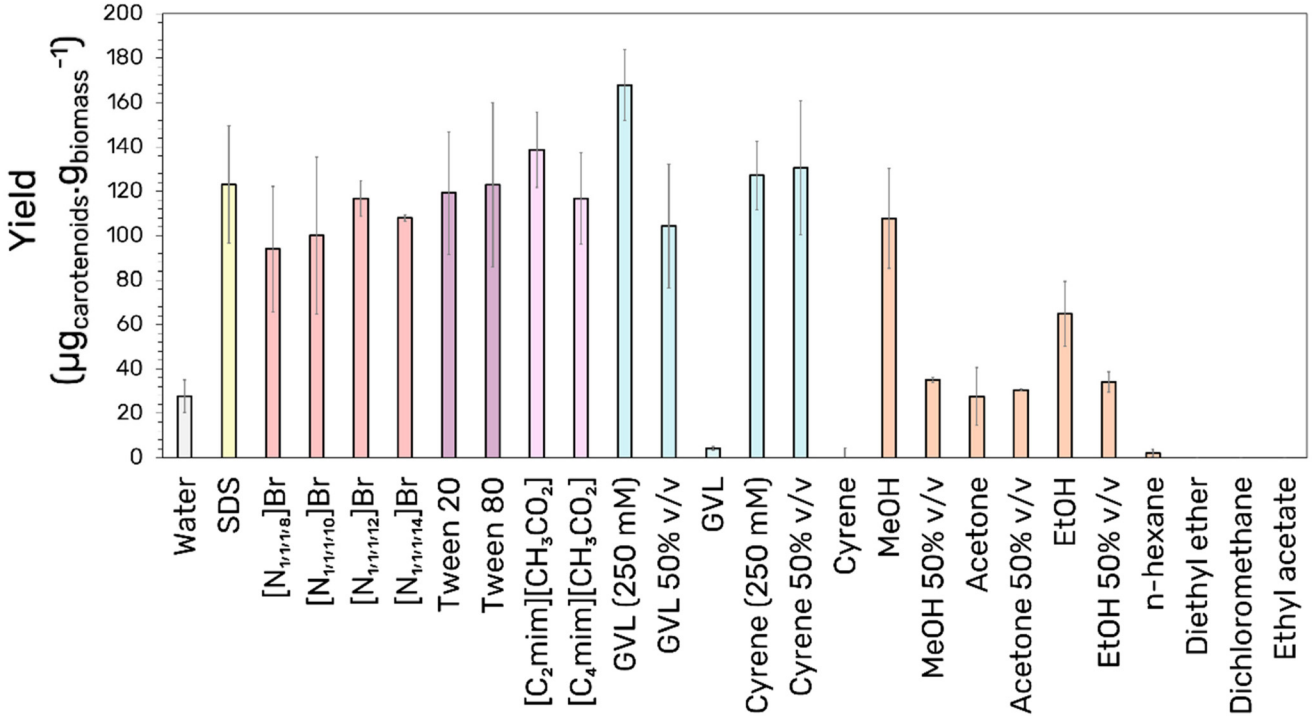

Fig. 1 Screening of different solvent families upon their ability to extract bacterioruberin from *H. salinarum* R1 (GVL – gamma-valerolactone, MeOH – methanol, EtOH – ethanol).

water (mM, *X*1), the solid–liquid ratio (SLR; *X*2), and the system pH (*X*3). This methodology allows for optimizing the response (bacterioruberin extraction yield) as a function of independent variables influencing the extraction yield and pigment stability. Twenty assays with six central (level 0) and axial points (−1.68 and +1.68 levels) were investigated in terms of bacterioruberin yield of extraction (in $\mu g_{bacterioruberin}\ g_{wet\ biomass}{}^{-1}$) (Table S1 in ESI†). The fitted model described in eqn (10), obtained using the analysis of variance (ANOVA) to estimate the statistical significance of the variables and their interactions, shows satisfying predictability at a confidence level of 95% with $R2 = 0.88$ and *F*-calculated > *F*-tabulated. The impact of these three variables on the bacterioruberin yield is illustrated in Fig. 2, in the Pareto chart in Fig. S3 and in the predicted-by-observed data plot depicted in Fig. S4, both in the ESI.†

$$\begin{aligned}\text{Yield of extraction}(mg_{bacterioruberin}\ g_{wet\ biomass}{}^{-1}) = 550.851 \\ - 29.423(X1) - 185.138(X1)2 + 33.384(X2) \\ - 28.516(X2)2 - 4.274(X3) - 204.484(X3)2 \\ + 28.137(X1) \times X2) - 6.687(X2) \times (X3)\end{aligned} \quad (10)$$

The response surfaces plotted in Fig. 2 show a small impact of the SLR on the yield of extraction when compared to the other variables. Advantageously, from a process perspective, an increase in SLR yielded better results at a maximum of 0.15, permitting the extraction to operate more intensively. The solvent concentration positively influences the extraction yield, with the maximum yield located at 150 mM, as seen in Fig. 2. The system's pH greatly influences the extraction process, where an optimum value was reached at pH = 7. This value is consistent with the reported lower stability of bacterioruberin for lower pH values (data not published). The model was validated after finding the optimal operational conditions (SLR 0.15, GVL 150 mM, and pH 7). A bacterioruberin yield of extraction of 531 ± 30 $\mu g_{carotenoids}\ g_{biomass}{}^{-1}$ was obtained experimentally, encompassing a mean relative deviation of 4 ± 1%, highlighting a high-predictive model.

The extraction kinetics was determined after determining the optimal parameters for pH, SLR, and GVL concentration (Fig. 3). The results demonstrate that maximum extraction is rapidly reached after 95 min, plateauing at 969 ± 40 $\mu g_{carotenoids}\ g_{biomass}{}^{-1}$.

By plotting t/C_t against t, the C_S and k_2 constants can be determined from the slope and intercept of the plot, respectively. The obtained parameters are summarized in Table 1 and indicate an improved fitting using the second-order model, yielding an extraction rate constant of $k_2 = 1.68 \times 10^{-4}\ g_{biomass}\ \mu g_{carotenoids}{}^{-1}\ min^{-1}$.

Protein and polysaccharide recovery

In-line with the ethos of a multiproduct biorefinery, the extracted bacterioruberin is purified from co-extracted proteins and polysaccharides to yield three separate fractions for valorization. Ethanol is frequently utilized as a precipitating agent due to its lower dielectric constant than water,[45] resulting in stronger attraction forces between proteins. Thus, 4 times the

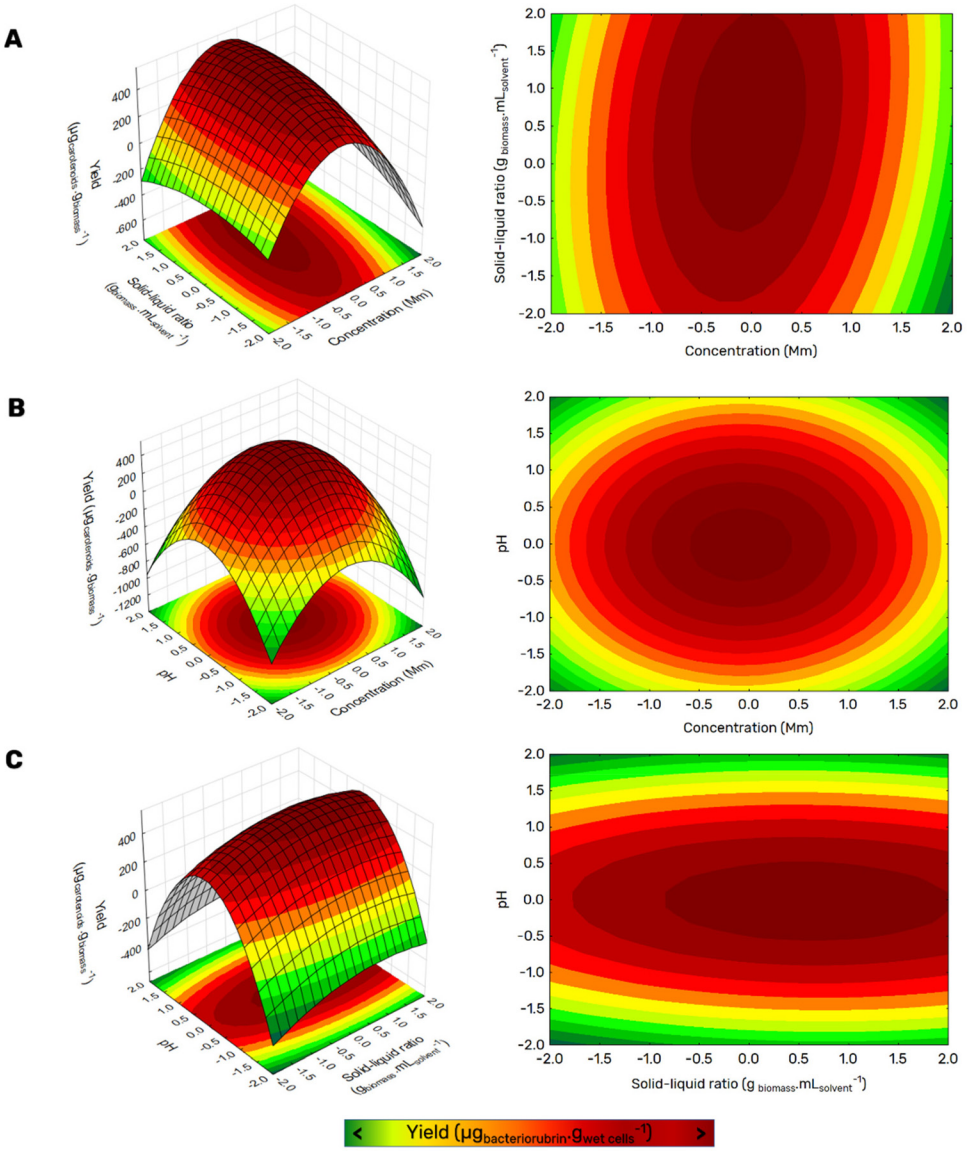

Fig. 2 Responsive surface and contour plots of the recovery yield of bacterioruberin from *H. salinarum* R1 as a function of (A) SLR and GVL concentration, (B) pH and GVL concentration, and (C) pH and SLR. SLR: solid–liquid ratio ($g_{biomass}$ $mL_{solvent}^{-1}$), concentration expressed in mM.

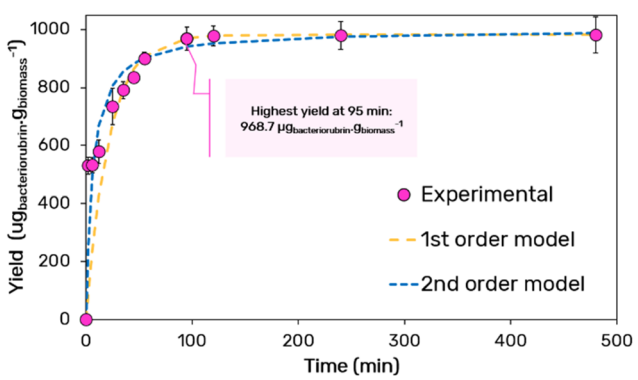

Fig. 3 Kinetic of bacterioruberin extraction along with the fitting obtained using the first and second-order kinetic models. All fitting parameters are summarized in Table 1.

Table 1 Linearization of the first and second-order kinetic models for bacterioruberin extraction for optimum conditions (pH = 7, SLR = 0.15 and [GVL] = 150 mM)

1st order model		2nd order model	
Slope	0.0471	Slope	0.0010
Intercept	0	Intercept	0.0060
r^2	0.986	r^2	0.999
C_S ($\mu g_{carotenoids}$ $g_{biomass}^{-1}$)	982	C_S ($\mu g_{carotenoids}$ $g_{biomass}^{-1}$)	1000
k_1 (min^{-1})	0.0471	k_2 ($g_{biomass}$ $\mu g_{carotenoids}^{-1}$ min^{-1})	0.000168

volume of ethanol was added to the extract to induce protein precipitation at 25 °C for 2 min. These conditions were chosen following a protocol previously described.[28] As depicted in

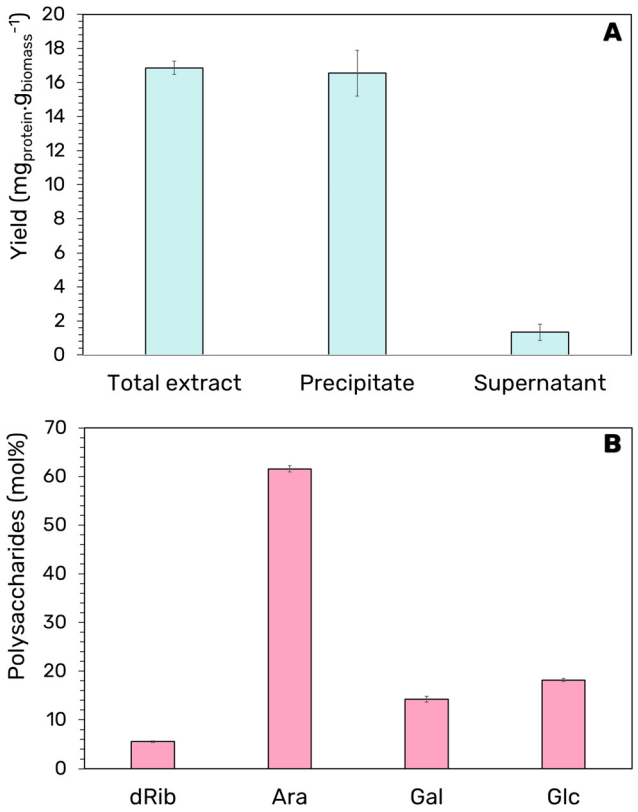

Fig. 4 (A) Protein partition in the precipitate and supernatant compared to the total extract concentration (t = 95 min, [GVL] = 150 mM, SLR = 0.15 and pH = 7) upon addition of ethanol (4 : 1 EtOH : extract v/v). The supernatant fraction here depicted expresses the amount of proteins in the polysaccharide-rich fraction. (B) Molar percentage of the polysaccharides-rich fraction (in PBS) after thermal precipitation of the proteins-rich fraction. dRib: D-ribose, Ara: arabinose, Gal: galactose, and Glc: glucose.

Fig. 4A, under these conditions, it was possible to recover an impressive 98% of the protein fraction concerning the total protein of the extract in a single step, corresponding to a yield of 16 ± 1 $mg_{protein}$ $g_{biomass}^{-1}$. Additionally, no co-precipitation of carotenoids was observed, confirming the complete separation of both fractions.

Separating the polysaccharides fraction to purify the protein fraction was also attempted. This would allow recovering a third product from this biorefinery proposal. Ethanol has been utilized not only for the precipitation of proteins but can also induce the precipitation of polysaccharides.[46] Thus, a second step was introduced to separate the polysaccharides and proteins from the ethanol-induced precipitation. Here, the pellet was resuspended in PBS to solubilize both hydrophilic products. Then, the samples were submitted to low temperature (4 °C for 24 h), which separated the two components by re-precipitation of the protein fraction, promoting the formation of a polysaccharide-rich fraction (as top phase). After, the liquid phase was analyzed by GC-MS to determine the relative proportion of the recovered carbohydrates. A total of 69.72 ± 4.40 $\mu g_{polysaccharides}$ mL^{-1} was recovered in the top phase. Besides, a low contamination of polysaccharides in the protein-rich fraction was achieved (7.80 ± 0.19%).

The composition analysis of the supernatant indicates that arabinose (Ara) makes up most of the recovered monosaccharides with approximately 60 mol% and lesser amounts of glucose (Glc), galactose (Gal), and D-ribose (dRib) (Fig. 4B). The four monosaccharides identified have potential as a platform for the development of chemicals, fuels, and food products. Arabinose, found in higher concentrations, has been studied as a pharmaceutical intermediate for anti-virus and anti-cancer drugs[18] and has shown prebiotic properties and blood sugar-lowering effects.[19] However, to date, the production costs have limited its application as a functional sweetener in food products.[47] This step allowed us to further valorize the biomass by recovering a carbohydrate-rich fraction enriched in a high-value monosaccharide with potential application in food products.

Stability and characteristic of the bacterioruberin extract

The antioxidant and colorant properties of the extracted bacterioruberin depend on its stability, as chemical and/or thermal degradation are known to influence biomolecules' color and biological potential. Although this can occur spontaneously under ambient conditions, natural pigments are particularly sensitive to increases in temperature.[48] Thus, it is essential to evaluate the bacterioruberin's stability under more aggressive, industrially relevant conditions, such as those required for pasteurization (0.5 min at 96 °C). The stability is further influenced by the presence of co-extracted cellular debris and by the solvent used. Therefore, the thermal stability of bacterioruberin was studied at three temperatures of 56 °C, 76 °C, and 96 °C for two conditions, namely after the optimized GVL extraction and after protein and polysaccharide precipitation *via* ethanol addition.

Table 2 shows the kinetic parameters calculated using the fitted data from the polynomial kinetic model obtained in Fig. 5. As expected, and independently of the degree of purity of bacterioruberin, raising temperature leads to a more significant decrease in the bacterioruberin half-life time ($t_{1/2}$). Notably, the decrease in the $t_{1/2}$ of bacterioruberin is smaller for the extracts after protein removal, further validating the proposed approach and the need for pigment purification. However, due to the change in the nature of the solvent mixture, it is unclear if the improved $t_{1/2}$ is solely due to the removal of the protein fraction or due to solvent effects. Nevertheless, upon protein precipitation, the $t_{1/2}$ was improved from 1732.9 min (28.9 h) to 2310.5 min (38.5 h) at 56 °C and, surprisingly, from 29.9 min (0.5 h) to 630.1 min (10.5 h) at 96 °C. In addition to the improved half-life time of bacterioruberin after purification, the pigment stability presents a decreased temperature dependency on its stability with an activation energy of E_A = 32.97 kJ mol^{-1}, three times lower than that obtained in the presence of proteins of E_A = 102.4 kJ mol^{-1}. This significant difference most likely reflects the different degradation pathways of bacterioruberin in both solvents.

Table 2 Influence of the presence of proteins and polysaccharides on the thermal stability of carotenoids (56 °C, 76 °C, and 96 °C)

	T = 56 °C		T = 76 °C		T = 96 °C		
Condition	K_d (min^{-1})	$t_{1/2}$ (min)	K_d (min^{-1})	$t_{1/2}$ (min)	K_d (min^{-1})	$t_{1/2}$ (min)	E_A (kJ mol^{-1})
Before protein precipitation	0.0004	1732.9	0.0032	216.6	0.0232	29.9	102.4
After protein precipitation	0.0003	2310.5	0.0007	990.1	0.0011	630.1	32.97

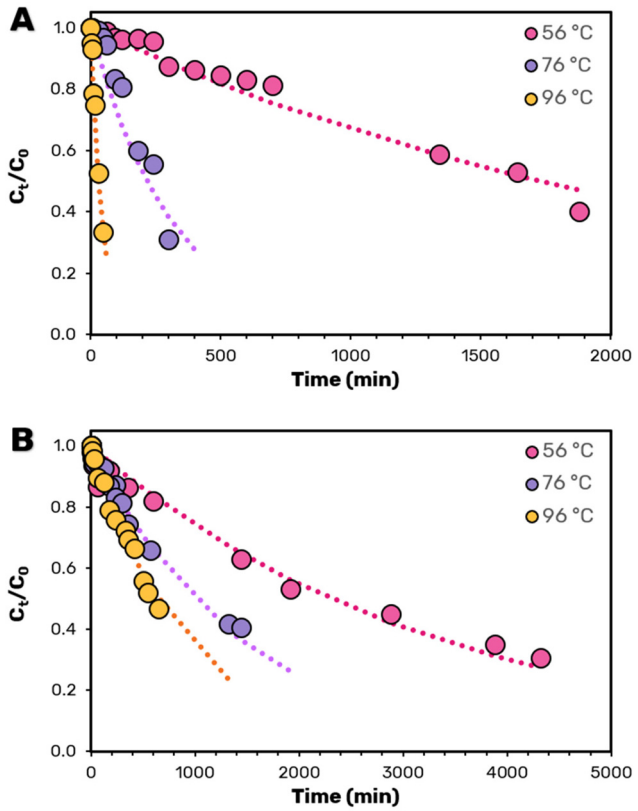

Fig. 5 (A) Kinetic curves for carotenoid degradation as a function of temperature in the GVL extract (A) before and (B) after protein precipitation through the addition of ethanol. Dashed lines correspond to the polynomial order kinetic fitting using the k_d values listed in Table 2.

While bacterioruberin is less stable in the presence of proteins, most likely through the formation of mixed aggregates, once thermal degradation is initiated, it occurs more rapidly as proteins are also thermo-sensitive such that their degradation could influence the stability of bacterioruberin. Regardless of the underlying mechanism, the stability results justify the purification of bacterioruberin, both from a multi-biorefinery perspective and the increased half-life of more valuable C_{50} pigment. Moreover, achieving a significant degree of purity enhances the product's value. It simplifies its application in situations requiring a pure compound and the production of chemical standards for analysis.

Process design and ecoscale

Following the individual optimization of each step, an integrated process is proposed, which enables the sequential recovery of three fractions (pigment, proteins, and polysaccharides) from *H. salinarum* R1 using a bio-based low-volatility solvent (GVL). The selection of GVL is crucial to reducing the environmental impact of the extraction process. The most valuable product recovered is bacterioruberin, a C50 carotenoid with high antioxidant activity.[49] Due to its properties and possible application in the pharmaceutical and cosmetic industries, GVL was considered as being part of an extract rich in bacterioruberin, without the need for solvent removal. A comprehensive diagram of the process contemplating all steps is proposed and presented in Fig. 6. In short, *H. salinarum* R1 is first cultured (cultivation of *H. salinarum* R1 – step I). After, wet cells are submitted to a solid–liquid extraction, where bacterioruberin is successfully extracted to the GVL-rich phase (solid–liquid extraction – step II). The extract is then contacted with 4× volume of ethanol, purifying the pigment by removing the proteins and polysaccharides, which precipitate (precipitation/purification – step III). The ethanol is then evaporated and re-incorporated into the process. This step emphasizes the focus on waste minimization and enhancement of the circular economy aspect within the biorefinery process.

Ultimately, the pigment extracted can be directly incorporated into various product formulations. Alternatively, ultrafiltration could separate GVL from the pigment and the extractant media re-utilized (solvent removal – step IV). Step IV is only needed when the presence of GVL is not allowed/desired in the final application. Fractionating both products further valorized the precipitated proteins and carbohydrates (step III). This separation was achieved by resuspending the pellet in PBS and submitting the solution to low temperature (4 °C) over 24 h, leading to the precipitation of the proteins fraction. The proteins are then recovered in a solid state, and the polysaccharides are recovered in an aqueous solution as secondary products. This pioneering work allowed us to extensively valorize the biomass by recovering three different products. The integrated biorefinery approach developed represents a sustainable design with economic feasibility. The environmental merit of the process is demonstrated through the Ecoscale analysis applied to three different commercial scenarios.

Scenario 1 involved the commercialization of bacterioruberin without precipitating proteins and polysaccharides and omitting solvent reuse (steps I and II). Scenario 2 included solvent precipitation and obtaining three refined products (bacterioruberin, proteins, and polysaccharides), without solvent reuse (steps I, II, and III). Lastly, scenario 3, the most comprehensive, encompassed all steps of the biorefinery process (steps I–IV), yielding the same three distinct products

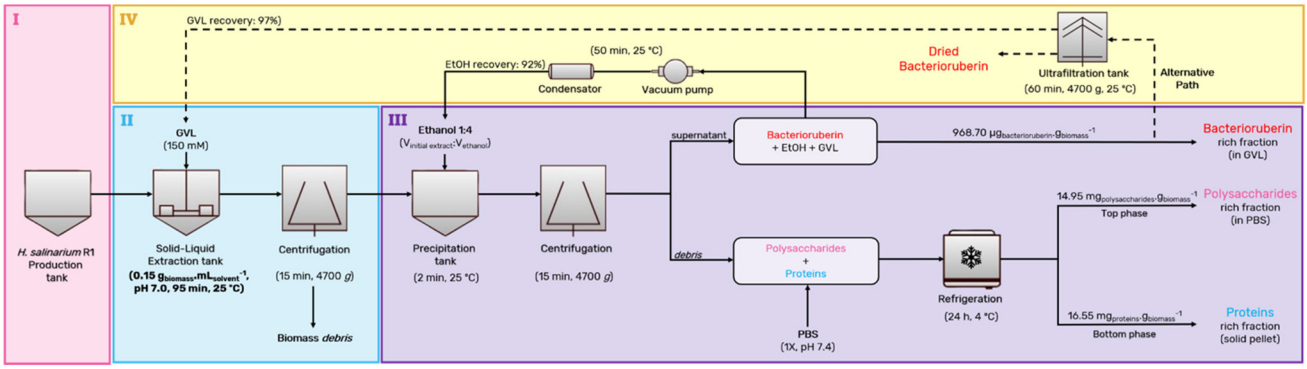

Fig. 6 Proposed integrated platform representing the multiproduct pipeline biorefinery of *H. salinarum* R1. The non-optimized aspects of the flowsheet are shown using dashed lines.

as scenario 2 but with solvent reuse. In scenario 3, the costs and benefits of recycling raw materials (primarily GVL and ethanol) were also simulated, showcasing the adaptability of the process towards maximizing the resource efficiency and sustainability. It is essential to highlight that steps I (*H. salinarum* R1 cultivation) and II (solid–liquid extraction) were considered mandatory, as they simultaneously generated the three products without purification.

The Ecoscale tool was used to assess the environmental impact of the biorefinery approach developed for *H. salinarum* R1 under each proposed economic scenario (scenarios I, II, and III cycle – 10). Additionally, it was applied to evaluate if our strategy aligns with the principles of green chemistry and compare it with other articles pursuing a similar objective of carotenoid extraction (the Ecoscale of those processes was hence also considered). Table 3 shows the Ecoscale of the biorefinery approach developed here, compared to the results of other works (some of those published by us). A deduction of 10 points in the safety parameter was applied to all processes using ethanol and other high-volatile organic solvents (as solvents or purification reagents) (Table 3). While ethanol is generally regarded as an environmentally friendly solvent widely employed in various industries, such as food and pharmaceuticals, it is also a volatile organic solvent. So, there are inherent risks associated with flammability and the generation of vapours, which can compromise both the safety of the manufacturing process and the quality of labor conditions.[48] Besides, two of the evaluated works used toluene and dichloromethane, suffering an additional penalty of five points. Indeed, these solvents are commonly used in various industries. However, both solvents could lead to respiratory problems, neurological disorders, and a systemic environmental impact.[50] Our process mitigates these risks by employing GVL, which does not incur safety penalties due to its lower volatility and reduced flammability, thus enhancing the safety profile of our manufacturing process. None of the evaluated studies was penalized in the "price/availability" parameter. This lack of penalties can be attributed to all the assessed works using the alternative solvent in low concentrations, typically in the millimolar range, within an aqueous or ethanolic solution. Despite the limited availability of these solvents on an industrial scale, it is feasible to produce several liters of extractant media with just a small initial quantity. Consequently, the price parameter did not result in any penalties for the evaluated works. Additionally, the extracts obtained through mild-homogenization approaches did not incur any penalties regarding the technical setup. However, ultrasound-assisted extraction (UAE) and techniques that involved solvent evaporation under vacuum incurred a penalty of one point. This aspect is due to these methods' higher energy requirements than the mild agitation operation modes.

The extraction process often requires energy-intensive operations such as heating, cooling, mixing, and separation. High energy consumption translates into higher operating costs and increased demand for resources. It also amplifies the environmental burden by depleting finite energy resources and contributing to environmental pollution associated with energy generation. Furthermore, the replacement of fossil by renewable energy, the choice of energy-efficient equipment, and process optimization can substantially reduce the environmental impact. Implementing energy-saving technologies, improving heat recovery systems, and optimizing process parameters can minimize energy waste and lower the overall carbon footprint of an extraction process.[51] Considering the significant impact of energy on the environmental footprint of the extraction processes, the Ecoscale database deducted 5 points for processes that require a significant reduction in temperature, such as those employing thermal precipitation as a purification strategy. This deduction reflects the recognition that these processes consume more energy, contributing to a larger environmental footprint. However, when considering the necessity to recycle the alternative solvents and the challenges involved in developing polishing strategies, what may initially seem like a disadvantage could turn into an advantage. By recovering and reusing the solvents, it becomes possible to perform new extraction cycles, thereby increasing the yield of high-value products and potential profits. This aspect showcases the potential of a long-term sustainable and econ-

Table 3 Penalty points assigned by the Ecoscale for the environmental analysis of each extraction scenario (I, II, and III – cycle 10) in the proposed biorefinery approach (*H. salinarum* R1), and a comparison with penalty points from other relevant studies. The penalty points reflect the environmental impact of each parameter, allowing for an assessment of their eco-friendliness and sustainability

Carotenoids source	Ref.	Yield ($\mu g_{carotenoids}\ g_{biomass}^{-1}$)	Relative yield[a] (%)	Reagents	Technical/setup	Price/ availability	Safety	Temperature/ time	Workup purification	Ecoscale
H. salinarum R1 (scenario III – cycle 10)	This work	9687.00[b]	100	GVL, water, EtOH	1 (solvent evaporation)	0	−10	−5 (thermal precipitation)	−2 (ultrafiltration)[c]	80.00
H. salinarum R1 (scenario II)	This work	968.70	10	GVL, water, EtOH	0	0	−10	−5 (thermal precipitation)		39.00
H. salinarum R1 (scenario I)	This work	968.70	10	GVL, water	0	0	0	0	0	55.00
Saccharina latissima	37	1956.00	20.19	$[P_{4,4,4,14}]Cl$, water, toluene	0	0	−15	0	−3 (liquid–liquid extraction)	42.10
Neochloris oleoabundans	52	1600.00	16.51	$[P_{4,4,4,14}]Cl$, water, PEG 8000, NaPa	0	0	0	0	−3 (aqueous biphasic system)	55.25
Bactris gasipaes wastes	16	1287.00	13.28	$[C_4mim][BF_4]$, water, EtOH	−1 (UAE)	0	−10	−5 (thermal precipitation)	−1 (crystalization)	38.64
Haloferax mediterranei ATCC 33500	28	370.00	3.81	Tween 20, EOH	−1 (solvent evaporation)	0	−10	−5 (thermal precipitation)	−1 (crystalization)	35.91
Bactris gasipaes wastes	53	354.80	3.66	$[N_{1,1,1,10}]Br$, water	0	0	0	0	0	51.83
Shrimp waste	54	92.70	0.95	$[C_4mim]Br$, EtOH, dichloromethane	−1 (UAE)	0	−15	0	−2 (solid-phase extraction)	32.47
Orange peels	55	32.08	0.33	$[C_4mim]Cl$, EtOH	−1 (UAE)	0		0	−2 (solid-phase extraction)	37.17
Tomatoes	56	8.00	0.082	$[C_4mim]Cl$, EtOH	−1 (UAE)	0	−10	−5 (thermal precipitation)	−1 (crystalization)	33.03

[a] Relative yield calculated by comparing the yields obtained in the other evaluated works. [b] Corresponding to 100% of the relative yield. [c] Once ultrafiltration is not present in the Ecoscale database, equivalent penalty points of solid-phase extraction was employed. GVL: gamma-valerolactone; EtOH: ethanol; $[P_{4,4,4,14}]Cl$: tributyltetradecylphosphonium chloride; NaPa: sodium polyacrylate; PEG 8000: polyethylene glycol 8000; Tween 20: polysorbate 20; UAE: ultrasound-assisted extraction; $[C_4mim][BF_4]$: 1-butyl-3-methylimidazolium tetrafluoroborate; $[N_{1,1,1,10}]Br$: decyltrimethylammonium bromide; $[C_4mim]Br$: 1-butyl-3-methylimidazolium bromide; $[C_4mim]Cl$: 1-butyl-3-methylimidazolium chloride.

omically viable approach, as scenario III – cycle 10 of the proposed biorefinery approach exemplifies. This scenario achieved the highest Ecoscale score, not only in comparison to other scenarios using the same biomass but also when compared to other published works, with an overall score of 80. It demonstrates the approach's effectiveness in terms of environmental impact and its competitive position among existing methodologies, besides the advantages of recycling raw materials. While this Ecoscale analysis primarily focuses on assessing the metrics of the technologies employed and solvent recirculation/reuse, it is important to highlight that other factors were inherently considered during the process development. Although this work primarily serves as a proof-of-concept with a predominant focus on product output, conscious efforts were made to minimize waste generation. Firstly, our process generates only one waste product: solid biomass residues after extraction and does not produce any liquid waste. Furthermore, our current Ecoscale evaluation represents a conservative estimate, potentially reflecting the highest environmental impact of our process. This is because any future integration of energy recycling or a switch to renewable energy sources would further enhance the sustainability of our process. Whenever possible, we opted for room temperature conditions (*e.g.*, in SLE) and maintained atmospheric pressure. We also used wet biomass, thus avoiding additional energy input associated with drying steps.

Economic viability

The economic viability of the biorefinery approach developed for *H. salinarum* R1 was assessed using the three commercial scenarios proposed before. Fig. 7 illustrates the percentage cost breakdown of each step in the biorefinery approach. Notably, solid–liquid extraction (step II) accounted for only 0.78% of the total cost, indicating the cost-effectiveness of the optimization techniques and extraction methods employed. Steps III and IV, with solvent recycling, offered the opportunity to generate protein and polysaccharide-rich fractions, enhancing the overall yield, economic returns, and environmental sustainability by fully valorizing the biomass. A recommended solvent removal step enabled the recovery of GVL and ethanol, facilitating their reuse in subsequent extraction cycles. This sequential extraction process using recycled raw materials allowed for the extraction of new products from a fresh batch of *H. salinarum* R1, increasing the yield of new products. Table S3 (ESI†) provides a comprehensive cost breakdown for the biorefinery approach, demonstrating that scenario III, with solvent recycling, proved to be more cost-effective compared to scenarios I and II. Moreover, after the third cycle, the production cost stabilized at $78.13. At the same time, returns increased due to acquiring new products using recycled raw materials, reaching $7859.31 after ten cycles with the same solvent. Despite the relatively low cost of GVL used in step II, recycling efforts proved economically advantageous, mainly as GVL could be considered a contaminant in specific applications and needs removal from the carotenoid extract. In addition, GVL costs could vary more than 100%, depending on the country where it is purchased. Thus, preliminary data on the economic viability of the proposed biorefinery demonstrates a promising scenario, especially when solvents are reused in subsequent extractions. Additionally, different α-scenarios were simulated, representing varying raw material prices (α = 0.1, 1, 5, and 10). Fig. S5 (ESI†) reveals that even with a 10-fold increase in raw material prices (most expensive scenario, α = 10), profits can be gained through their reuse, thereby increasing profits in each extraction cycle, highlighting the economic viability of our biorefinery approach. This scenario is not only economically sound but also environmentally robust, boasting the highest Ecoscale score and showcasing its superior performance compared to existing techniques.

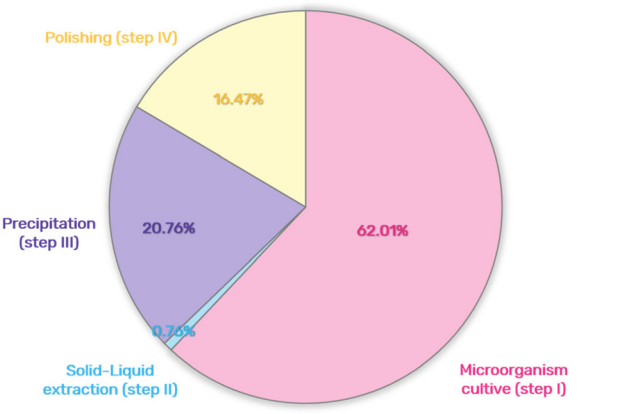

Fig. 7 Contributions of the costs (US$) of each step of the biorefinery developed.

Conclusions

This study presents a holistic approach to designing a biorefinery to efficiently utilize various fractions obtained from *H. salinarum* R1, focusing on maximizing the recovery of bacterioruberin—the molecule with highest commercial value. The proposed methodology encompasses the optimal disruption of *H. salinarum* R1 cells, extraction of diverse biomolecules, fractionation of compounds, isolation of target molecules, and incorporation of solvent recycling processes. Indeed, solvent recycling is not mandatory once the operation cost is quite inexpensive. However, suppose the final application intends to recover pure carotenoids without solvent. In that case, we also propose a solvent removal step, being possible to recycle all the raw materials used in the biorefinery approach. In this work, an extensive screening of solvents (conventional and alternatives) from different classes was conducted, and a dilute aqueous mixture of GVL at a concentration of 250 mM was ultimately selected as the extraction medium due to its superior ability to recover bacterioruberin. The process variables were optimized, and the optimal operating conditions were determined: GVL concentration in water at 150 mM, SLR of 0.15, and pH 7. The kinetics of the extraction

yield were also evaluated, and a maximum yield of 968 $\mu g_{carotenoids}\ g_{biomass}^{-1}$ was achieved after 95 minutes. The thermal stability of the pigment was also evaluated, showing that purified carotenoids are more thermally stable than the mixture of carotenoids with macronutrients, which justified a purification approach to separate carotenoids from proteins and polysaccharides, increasing the price of the obtained carotenoid and obtaining two more high-added products. Thus, the recovery of the proteins and carbohydrates co-extracted with the pigment was achieved using induced ethanol precipitation, followed by temperature-based fractionation. In the end, this work produced three ready-to-market products, demonstrating the application of an integrated biorefinery approach for treating archaea and paving the way for valorizing this unique class of marine biomass.

Conflicts of interest

The authors declare that they have no known competing financial interests or personal relationships that could have appeared to influence the work reported in this paper.

Acknowledgements

This work was supported by "Fundação de Amparo à Pesquisa do Estado de São Paulo – FAPESP" through the projects (2018/14582-5 and 2019/13496-0) and fellowships (L. M. de S. M.: 2020/08421-9, 2021/11022-1; LCS: 2020/03623-2, 2021/11023-8). This work was supported by Conselho Nacional de Desenvolvimento Científico e Tecnológico (CNPq, Brazil) (productivity grant 302610/2021-9). This work was developed within the scope of the project CICECO-Aveiro Institute of Materials, UIDB/50011/2020, UIDP/50011/2020 & LA/P/0006/2020, financed by national funds through the FCT/MEC (PIDDAC). The authors acknowledge FTC/MCTES for the financial support to CESAM, UIDB/50017/2020 + UIDP/50017/2020 + LA/P/0094/2020, financed by national funds. The authors are also grateful to the FCT for the doctoral grants of M. Kholany (SFRH/BD/138413/2018), I. P. E. Macário (SFRH/BD/123850/2016), and T. Veloso (SFRH/BD/147346/2019). The National NMR Network, funded within the frame-work of the National Program for Scientific Re-equipment, contract REDE/1517/RMN/2005 with funds from POCI 2010 (FEDER) and FCT, is also acknowledged. CN is grateful to Portuguese national funds (OE), through FCT, I.P., in the scope of the framework contract foreseen in the numbers 4, 5 and 6 of the article 23, of the Decree-Law 57/2016, of August 29, changed by Law 57/2017, of July 19.

References

1 J. B. Zimmerman, P. T. Anastas, H. C. Erythropel and W. Leitner, *Science*, 2020, **367**, 397–400.
2 P. Stegmann, M. Londo and M. Junginger, *Resour., Conserv. Recycl. X*, 2020, **6**, 100029.
3 K. Pfeifer, İ. Ergal, M. Koller, M. Basen, B. Schuster and S. K. M. R. Rittmann, *Biotechnol. Adv.*, 2021, **47**, 107668.
4 S. Daniotti and I. Re, *Mar. Drugs*, 2021, **19**, 61.
5 T. Suganya, M. Varman, H. H. Masjuki and S. Renganathan, *Renewable Sustainable Energy Rev.*, 2016, **55**, 909–941.
6 K. R. Biazotto, L. M. De Souza Mesquita, B. V. Neves, A. R. C. Braga, M. M. P. Tangerina, W. Vilegas, A. Z. Mercadante and V. V. De Rosso, *J. Agric. Food Chem.*, 2019, **67**, 1860–1876.
7 M. Giani, I. Garbayo, C. Vílchez and R. M. Martínez-Espinosa, *Mar. Drugs*, 2019, **17**, 524.
8 M. Rodrigo-Baños, I. Garbayo, C. Vílchez, M. J. Bonete and R. M. Martínez-Espinosa, *Mar. Drugs*, 2015, **13**, 5508.
9 F. Mandelli, V. S. Miranda, E. Rodrigues and A. Z. Mercadante, *World J. Microbiol. Biotechnol.*, 2012, **28**, 1781–1790.
10 L. M. De Souza Mesquita, L. V. Mennitti, V. V. De Rosso and L. P. Pisani, *Nutr. Rev.*, 2021, **79**, 76–87.
11 M. Kottemann, A. Kish, C. Iloanusi, S. Bjork and J. DiRuggiero, *Extremophiles*, 2005, **9**, 219–227.
12 C. J. Clarke, W. C. Tu, O. Levers, A. Bröhl and J. P. Hallett, *Chem. Rev.*, 2018, **118**, 747–800.
13 R. H. Wijffels, M. J. Barbosa and M. H. M. Eppink, *Biofuels, Bioprod. Biorefin.*, 2010, **4**, 287–295.
14 G. P. 't Lam, M. H. Vermuë, M. H. M. Eppink, R. H. Wijffels and C. van den Berg, *Trends Biotechnol.*, 2018, **36**, 216–227.
15 K. T. Amorim-Carrilho, A. Cepeda, C. Fente and P. Regal, *TrAC, Trends Anal. Chem.*, 2014, **56**, 49–73.
16 L. M. De Souza Mesquita, S. P. M. Ventura, A. R. C. Braga, L. P. Pisani, A. C. R. V. Dias and V. V. De Rosso, *Green Chem.*, 2019, **21**, 2380–2391.
17 S. Khanra, M. Mondal, G. Halder, O. N. Tiwari, K. Gayen and T. K. Bhowmick, *Food Bioprod. Process.*, 2018, **110**, 60–84.
18 Q. Liu, N. Li and Y. Shen, *IERI Proc.*, 2013, **5**, 70–74.
19 K. Pol, M.-L. Puhlmann and M. Mars, *Foods*, 2022, **11**, 157.
20 R. Katiyar, S. Banerjee and A. Arora, *Biofuels, Bioprod. Biorefin.*, 2021, **15**, 879–898.
21 M. H. M. Eppink, S. P. M. Ventura, J. A. P. Coutinho and R. H. Wijffels, *Trends Biotechnol.*, 2021, **39**, 1131–1143.
22 P. Cheng, Y. Li, C. Wang, J. Guo, C. Zhou, R. Zhang, Y. Ma, X. Ma, L. Wang, Y. Cheng, X. Yan and R. Ruan, *Sci. Total Environ.*, 2022, **817**, 152895.
23 F. A. Vicente, S. P. M. Ventura, H. Passos, A. C. R. V. Dias, M. A. Torres-Acosta, U. Novak and B. Likozar, *Chem. Eng. J.*, 2022, **442**, 135937.
24 C. J. Clarke, W. C. Tu, O. Levers, A. Bröhl and J. P. Hallett, *Chem. Rev.*, 2018, **118**, 747–800.
25 R. K. Saini and Y. S. Keum, *Food Chem.*, 2018, **240**, 90–103.
26 L. Zalazar, P. Pagola, M. V. Miró, M. S. Churio, M. Cerletti, C. Martínez, M. Iniesta-Cuerda, A. J. Soler, A. Cesari and R. De Castro, *J. Appl. Microbiol.*, 2019, **126**, 796–810.
27 M. Abbes, H. Baati, S. Guermazi, C. Messina, A. Santulli, N. Gharsallah and E. Ammar, *BMC Complementary Altern. Med.*, 2013, **13**, 1–8.
28 B. M. C. Vaz, M. Kholany, D. C. G. A. Pinto, I. P. E. Macário, T. Veloso, T. Caetano, J. L. Pereira, J. A. P. Coutinho and S. P. M. Ventura, *RSC Adv.*, 2022, **12**, 30278–30286.

29 F. Kerkel, M. Markiewicz, S. Stolte, E. Müller and W. Kunz, *Green Chem.*, 2021, **23**, 2962–2976.
30 I. T. Horváth, H. Mehdi, V. Fábos, L. Boda and L. T. Mika, *Green Chem.*, 2008, **10**, 238–242.
31 European Commission, COSING Database [Gamma-Valerolactone], **https://ec.europa.eu/growth/tools-databases/cosing/details/41281**.
32 U.S. Food and Drug Administration, Substances Added to Food [Gamma-Valerolactone], **https://www.cfsanappsexternal.fda.gov/scripts/fdcc/index.cfm?set=FoodSubstances&id=VALEROLACTONE**.
33 S. V. Kalenov, M. M. Baurina, D. A. Skladnev and A. Y. Kuznetsov, *J. Biotechnol.*, 2016, **233**, 211–218.
34 H. S. Kusuma and M. Mahfud, *RSC Adv.*, 2017, **7**, 1336–1347.
35 D. Balli, M. Khatib, L. Cecchi, A. Adessi, P. Melgarejo, C. Nunes, M. A. Coimbra and N. Mulinacci, *Food Chem.*, 2022, **397**, 133550.
36 L. M. de Souza Mesquita, F. H. B. Sosa, L. S. Contieri, P. R. Marques, J. Viganó, J. A. P. Coutinho, A. C. R. V. Dias, S. P. M. Ventura and M. A. Rostagno, *Food Chem.*, 2023, **406**, 135093.
37 M. Martins, L. M. D. S. Mesquita, B. M. C. Vaz, A. C. R. V. Dias, M. A. Torres-Acosta, B. Quéguineur, J. A. P. Coutinho and S. P. M. Ventura, *ACS Sustainable Chem. Eng.*, 2021, **9**, 6599–6612.
38 K. Van Aken, L. Strekowski and L. Patiny, *Beilstein J. Org. Chem.*, 2006, **2**, 3.
39 M. Kholany, P. Trébulle, M. Martins, S. P. M. Ventura, J. M. Nicaud and J. A. P. Coutinho, *J. Chem. Technol. Biotechnol.*, 2020, **95**, 1126–1134.
40 B. Li, J. Wang, M. E. Moustafa and H. Yang, *ACS Biomater. Sci. Eng.*, 2019, **5**, 6355–6360.
41 A. F. M. Cláudio, M. C. Neves, K. Shimizu, J. N. Canongia Lopes, M. G. Freire and J. A. P. Coutinho, *Green Chem.*, 2015, **17**, 3948–3963.
42 D. O. Abranches, J. Benfica, S. Shimizu and J. A. P. Coutinho, *Ind. Eng. Chem. Res.*, 2020, **59**, 18247–18253.
43 H. Tian, C. Xu, J. Cai and J. Xu, *J. Chem. Thermodyn.*, 2018, **125**, 41–49.
44 D. O. Abranches, J. Benfica, S. Shimizu and J. A. P. Coutinho, *Ind. Eng. Chem. Res.*, 2020, **59**, 18649–18658.
45 S. He, B. Cao, Y. Yi, S. Huang, X. Chen, S. Luo, X. Mou, T. Guo, Y. Wang, Y. Wang, G. Yang and C. Yanwei Wang, *Nano Sel.*, 2022, **3**, 617–626.
46 J. Xu, R. Q. Yue, J. Liu, H. M. Ho, T. Yi, H. B. Chen and Q. Bin Han, *Int. J. Biol. Macromol.*, 2014, **67**, 205–209.
47 B. Hu, H. Li, Q. Wang, Y. Tan, R. Chen, J. Li, W. Ban and L. Liang, *World J. Eng. Technol.*, 2018, **6**, 24–36.
48 L. M. de Souza Mesquita, L. S. Contieri, F. H. B. Sosa, R. S. Pizani, J. Chaves, J. Viganó, S. P. M. Ventura and M. A. Rostagno, *Green Chem.*, 2023, **25**, 1884–1897.
49 A. T. Caimi, O. Yasynska, P. C. Rivas Rojas, E. L. Romero and M. J. Morilla, *J. Drug Delivery Sci. Technol.*, 2022, **77**, 103896.
50 H. Deng, T. Pan, Y. Zhang, L. Wang, Q. Wu, J. Ma, W. Shan and H. He, *Chem. Eng. J.*, 2020, **394**, 124986.
51 M. J. B. Kabeyi and O. A. Olanrewaju, *Front. Energy Res.*, 2022, **9**, 743114.
52 B. M. C. Vaz, M. Martins, L. M. de Souza Mesquita, M. C. Neves, A. P. M. Fernandes, D. C. G. A. Pinto, M. G. P. M. S. Neves, J. A. P. Coutinho and S. P. M. Ventura, *Chem. Eng. J.*, 2022, **428**, 131073.
53 L. M. de Souza Mesquita, M. Martins, É. Maricato, C. Nunes, P. S. G. N. Quinteiro, A. C. R. V. Dias, J. A. P. Coutinho, L. P. Pisani, V. V. de Rosso and S. P. M. Ventura, *ACS Sustainable Chem. Eng.*, 2020, **8**, 4085.
54 W. Bi, M. Tian, J. Zhou and K. H. Row, *J. Chromatogr. B*, 2010, **878**, 2243.
55 D. C. Murador, A. R. C. Braga, P. L. G. Martins, A. Z. Mercadante and V. V. de Rosso, *Food Res. Int.*, 2019, **126**, 108653.
56 P. L. G. Martins and V. V. de Rosso, *Food Res. Int.*, 2016, **82**, 156.